

UC Santa Barbara

UC Santa Barbara Previously Published Works

Title

Gas exchange rates in the tidal Hudson river using a dual tracer technique

Permalink

<https://escholarship.org/uc/item/44k924mq>

Journal

Tellus B, 46(4)

ISSN

0280-6509

Authors

Clark, Jordan F
Wanninkhof, Rik
Schlosser, Peter
[et al.](#)

Publication Date

2023-05-31

DOI

10.3402/tellusb.v46i4.15802

Peer reviewed

Gas exchange rates in the tidal Hudson river using a dual tracer technique

By JORDAN F. CLARK^{1*}, RIK WANNINKHOF², PETER SCHLOSSER¹ and H. JAMES SIMPSON¹, ¹*Lamont-Doherty Earth Observatory, Department of Geological Sciences, Columbia University, Palisades, NY 10964, USA;* ²*Ocean Chemistry Division, NOAA/AOML, Miami, FL 33149, USA*

(Manuscript received 13 January 1994; in final form 6 May 1994)

ABSTRACT

Gas exchange rates have been determined in the tidal Hudson River by injecting 2 inert gases, ³He and sulfur hexafluoride (SF₆) and monitoring their decline with time. Their distributions along the main axis of the river were approximately gaussian and maximum concentrations of excess ³He and SF₆ observed during each transect decreased from about 6500 × 10⁻¹⁶ cm³ STP g⁻¹ and 250 ppt (part per trillion by volume), respectively, to values close to atmospheric equilibrium concentrations over a period of 16 days. Throughout the experiment, vertical gradients in tracer concentration were observed. After 3 days of mixing, tracer concentrations in bottom samples were 0–19% greater than in surface samples. Gas transfer velocities were calculated from the temporal change in the depth averaged excess ³He/SF₆ ratio from stations having maximum tracer concentrations. They ranged from 1.5 to 9.0 cm h⁻¹ and correlated well with mean wind speed.

1. Introduction

The gas exchange rate across the air–water interface is a critical parameter needed to understand the dynamics of volatile substances in aqueous environments. While gas exchange rates have been studied extensively in the open ocean, lakes, and streams, very few direct measurements of this parameter in estuaries exist. Yet, the gas exchange rate is critical for the calculation of reaeration rates, fluxes of trace gases, and evasion rates of volatile contaminants (Juliano, 1969; Dyrssen et al., 1990; Thomann et al., 1991; Howarth et al., 1992; De Angelis and Scranton, 1993).

Several tracer methods which have been used successfully in the open ocean are not suited for estuaries. The ²²²Rn-deficit method (Peng et al., 1979), which calculates gas exchange rates from the degree of ²²²Rn disequilibrium from ²²⁶Ra

production has not worked in estuaries because of large ²²²Rn fluxes from sediments (Hammond et al., 1977). Bomb and natural radiocarbon methods (Broecker et al., 1985) are inappropriate because of the long half-life of ¹⁴C compared with the flushing rate of estuaries. Purposeful additions of a single tracer which has worked in lakes (Wanninkhof et al., 1985, 1987; Upstill-Goddard et al., 1990) is also not suited for estuaries because of the strong dispersion generated by the tidal circulation.

Most experiments which determined the gas exchange rate in estuaries have used the “helmet” method (Juliano, 1969; Hartman and Hammond, 1984; Marino and Howarth, 1993). With this method, the gas exchange rate is calculated from the accumulation rate of a gas into an inverted dome which floats upon the surface of the water. The problem with this method is the degree to which the floating dome disturbs the surface turbulence regime; the physical driving force behind gas exchange, is unknown. Laboratory experiments have found little agreement between

* Corresponding author.

gas exchange rates determined by the helmet method and other approaches (Stephens, 1978; Belanger and Korzum, 1991).

Other methods used to determine gas exchange rates in estuaries include the use of mass balance calculations (Juliano, 1969; Hartman and Hammond, 1984), disturbed equilibrium (Juliano, 1969), and volatile contaminant distributions (Clark et al., 1992). The weaknesses of these methods are that the magnitude and variability of sources and sinks of the dissolved gas must be well known. Uncertainties associated with these terms are passed on to the calculated gas exchange rate.

A new method to quantify gas exchange rates has recently been developed which can be used in tidal systems. The purposeful addition of two inert gases, ^3He and sulfur hexafluoride (SF_6), allows for calculation of gas exchange rates in aqueous systems where dispersion is strong (Watson et al., 1991; Wanninkhof et al., 1993). Because these gases are both biologically and chemically non-reactive in natural waters, transfer across the air-water interface should be the only process which removes these gases from solution. The method does not disturb the surface turbulence field and thus should be free of the type of uncertainties associated with the helmet experiments.

Here, we present the results of a gas exchange experiment which was carried out in the tidal fresh Hudson River using the ^3He - SF_6 method to assess the feasibility of this method in estuaries. Anemometers were placed within the river channel close to the tracer injection point to determine the relationship between gas exchange rate and wind speed.

2. Principle of the ^3He - SF_6 method

The theory of the ^3He - SF_6 method of determining gas exchange rates has been presented in detail elsewhere (Watson et al., 1991; Wanninkhof et al., 1993). Briefly, the gas transfer velocity, k , is defined in the following manner:

$$k = F / (C_{\text{sur}} - C_{\text{eq}}), \quad (1)$$

where F is the mass flux of gas across the air-water interface, C_{sur} and C_{eq} are the concentrations of

the gas in the water at the air-water interface and in equilibrium with the atmosphere, respectively.

Dilution and first-order decay of a pulse of tracer in one-dimensional systems such as exists in many tidal rivers has been described by O'Loughlin and Bowmer (1975). Gas transfer is a first order process. Solving the advection-diffusion equation with first order decay for two gases, ^3He and SF_6 , assuming that the first order gas transfer rates, $K_{^3\text{He}}$ and K_{SF_6} , are related by:

$$K_{\text{SF}_6} / K_{^3\text{He}} = (Sc_{(\text{SF}_6)} / Sc_{(^3\text{He})})^{-n} \quad (2)$$

leads to the following expression for the first order gas transfer rate of ^3He

$$K_{^3\text{He}} = \frac{d}{dt} \left(\frac{\ln([^3\text{He}] / [\text{SF}_6])}{1 - (Sc_{(\text{SF}_6)} / Sc_{(^3\text{He})})^{-n}} \right), \quad (3)$$

where $Sc_{(^3\text{He})}$, and $Sc_{(\text{SF}_6)}$ are the Schmidt numbers for ^3He and SF_6 calculated using the relationships given by Wanninkhof (1992), $[^3\text{He}]$ and $[\text{SF}_6]$ are the differences between the observed and atmospheric equilibrium concentrations for ^3He and SF_6 , respectively, and n is the Schmidt number exponent. The Schmidt number is defined as the kinematic viscosity of water divided by the molecular diffusion coefficient of the gas in water. For wavy surfaces not broken by white caps, n has been determined to be $\frac{1}{2}$ in both laboratory and field experiments (Jähne et al., 1987; Watson et al., 1991).

The mass flux of a gas can be calculated from the first order gas transfer rate in the following manner:

$$F = hK(C_m - C_{\text{eq}}) \quad (4)$$

where h is the mean water depth and C_m is the mean concentration of the gas in the water. Combining equations (1) and (4) leads to the following expression of the gas transfer velocity:

$$k = h \frac{(C_m - C_{\text{eq}})}{(C_{\text{sur}} - C_{\text{eq}})} K. \quad (5)$$

In systems that are vertically well mixed, the surface and mean concentrations are equal and the gas transfer velocity is equivalent to the mean depth multiplied by the first order gas transfer rate.

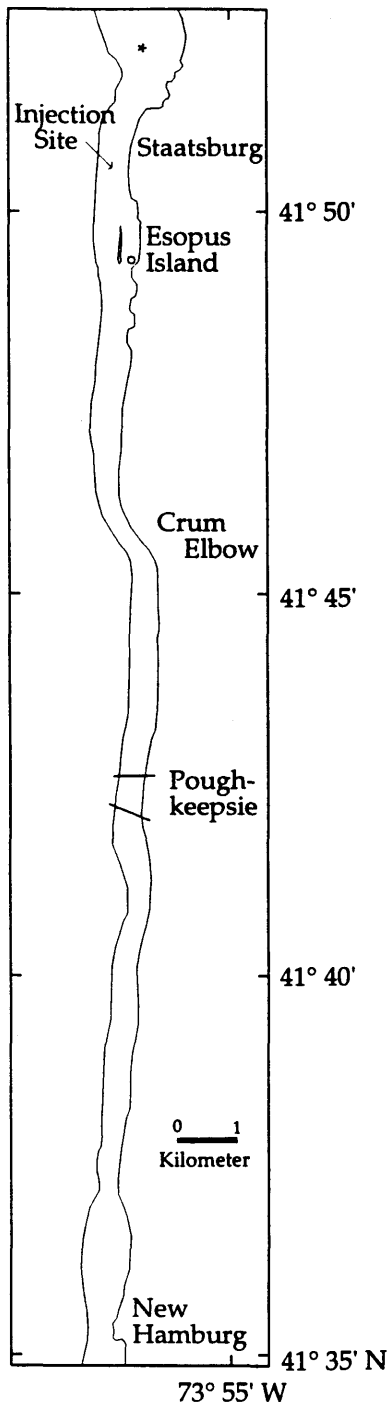


Fig. 1. Map of the portion of the Hudson river used in the tracer experiment. * marks the location of the Esopus Meadow Lighthouse and \circ marks the approximate location of the buoy.

3. Study location

The 30 km reach of the Hudson River between New Hamburg, NY, and Staatsburg, NY, located about 120 km north of New York harbor, has a very simple geometry (Fig. 1). The channel runs due south from Staatsburg to Crum Elbow where it jogs briefly to the east and then continues due south to New Hamburg. No major tributaries enter and no extended area of shallow water occurs along this stretch of river. The geometry is complicated only by Esopus Island which lies about 4 km south of Staatsburg. Tidal stage changes range from 0.8–1.4 m along this reach and mean tidal current velocities are 0.38 m s^{-1} (Limburg et al., 1986). During each tidal cycle, water masses move north and south about 10 km (Limburg et al., 1986). We have estimated the mean depth of the channel in this 30 km reach to be 14 m and the mean width to be 800 m using USGS and NOAA maps. Our estimate of the mean depth is greater than those reported for this general area by Deck (1981, 11 m) and Howarth et al. (1992, 9 m). However, both of these authors included the extensive shallows near and north of the Esopus Meadow Lighthouse in determining the mean depth. Our gas exchange tracer experiment was conducted downstream of this region of shallow water. Saline water is advected north of New Hamburg only during extended periods of low freshwater discharge. During the period of our tracer experiment, saline water was not observed in this reach of the Hudson.

4. Method

Prior to the tracer injection, about 0.045 moles of 99.8% pure ^3He gas and 31 moles of pure SF_6 gas were mixed into a large cylinder (43.8 l) in the laboratory. During the morning of 24 August 1993, approximately 0.6 moles of this mixture was injected through two diffusing stones into the tidal Hudson River about 3 km north of Esopus Island (see Fig. 1). The diffusing stones were attached to a 10 m rope which was suspended from a buoy. The gas mixture was injected over a period of about 20 min as the buoy was towed about 8 m behind a boat which crossed the channel twice. Because of drag caused by the rope and diffusion stones, the injection depth of the gas mixture was

shallower than 10 m. The injection took place during the first hour after slack high tide as the current was flowing to the south.

For approximately 16 days, at either slack high or slack low tide, samples were collected in sequence along the axis of the river from a small boat every 1 to 2 days using a 1.5 l Niskin bottle. Stations were spaced at intervals of 1 to 2 km. At each station, samples were collected about 1 m below the surface of the water and about 1 m above the sediments. Station locations were determined using a field Global Positioning System unit.

SF₆ samples were collected in either 50 ml glass syringes or 60 ml BOD bottles and stored submerged in water to minimize diffusional loss. All samples were analyzed within 12 h of collection using the head space method described by Wanninkhof et al. (1987). Briefly, the glass syringes were emptied (or filled) to a predetermined volume of water and then a head space was created with a known volume of nitrogen. After 3 min of shaking to equilibrate the N₂ with the water sample (more than 99% of the SF₆ is partitioned into the gas phase at room temperature), the head space gas was injected through a column of Mg(ClO₄)₂ into a small sample loop of known volume. Subsequently, the gas in the sample loop was flushed into a gas chromatograph equipped with an electron capture detector with high purity N₂ carrier gas. SF₆ was separated from other gases with a molecular sieve 5a column held at room temperature. Error on duplicate measurements was ±2% for samples having SF₆ concentrations greater than 10 ppt and ±0.5 ppt for samples with SF₆ concentrations less than 10 ppt.

About 40 ml of water was collected in copper tubes which were sealed by pinch-off clamps at each end for ³He analysis. Helium and other gases were transferred from copper tubes to glass ampoules containing activated charcoal using a vacuum extraction system. Prior to introduction into a VG-5400 helium isotope mass spectrometer, the helium was separated from all other gases by a series of cold traps. ⁴He was measured using a Faraday Cup and ³He was measured using a Johnston-MM1 electron multiplier. Throughout each day, air standards were run to calibrate the He isotope measurements. ⁴He concentration and ³He/⁴He ratio measurement errors were about ±0.5% and ±0.2%, respectively.

Excess ³He concentration was calculated from the measured ³He/⁴He ratio and ⁴He concentration in the following manner:

$$\begin{aligned} \text{excess } ^3\text{He} = & [^4\text{He}]_s (R_s - R_a) \\ & + [^4\text{He}]_{\text{eq}} R_a (1 - \alpha), \end{aligned} \quad (6)$$

where [⁴He]_s is the measured ⁴He concentration; [⁴He]_{eq} is the concentration of ⁴He in water which is in solubility equilibrium with the atmosphere calculated after Weiss (1971); R_s is the measured ³He/⁴He ratio; R_a is the atmospheric ³He/⁴He ratio (1.386 × 10⁻⁶, Clarke et al., 1976); and α is the solubility isotope effect (0.983, Benson and Krause, 1980).

Two anemometers were placed within the river channel (Fig. 1). One was placed on top of the Esopus Meadow Lighthouse 16 m above the high water mark. The lighthouse is about 600 m from the western shore and about 3 km north of the injection point. The second anemometer was placed 2.0 m above the surface of the water on a buoy which was moored in the Poughkeepsie Yacht Club anchorage about 2.5 km south of the injection point. The buoy was about 150 m from the eastern shore. Both anemometers recorded hourly mean wind speeds; the anemometer on the lighthouse also recorded prevailing wind direction using 16 compass directions. After the tracer experiment was over, the buoy was moved to the lighthouse to determine the vertical gradient of the wind speed.

Water and air temperatures were recorded hourly at the buoy.

5. Experimental results

5.1. Tracer distribution

SF₆ was not detected in water samples which were collected from the Hudson River in the area of the tracer experiment 6 weeks, 3 weeks, and 2 days prior to injection. ³He samples collected 2 days before the injection were in solubility equilibrium with the atmosphere (excess ³He = 0.5 ± 0.5 × 10⁻¹⁶). Throughout the experiment, ⁴He concentrations were equal to 4.54 ± 0.08 × 10⁻⁸ cm³ STP g⁻¹, approximately 3% greater than the atmospheric equilibrium value (4.40 × 10⁻⁸ cm³ STP g⁻¹ at 26°C; Weiss, 1971).

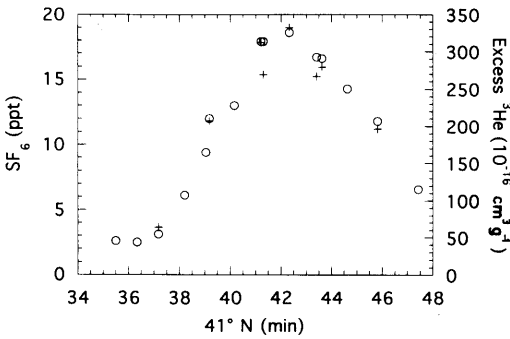


Fig. 2. Distribution of SF₆ and excess ³He on 31 August at slack low tide about 7 days after the injection. Open circles = SF₆ and crosses = excess ³He (no distinction has been made between surface and bottom samples).

After the injection, daily distributions of the tracer patches were approximately gaussian (Fig. 2). The patch grew from the injection "line" to more than 30 km long by the end of the experiment. Maximum concentrations observed during each day's sampling, the peak concentration, decreased systematically with time (Fig. 3a, Table 1). During each transect, the peak concentrations were represented by only one station. Except for day 4.2, the SF₆ peak was always found coincident with the ³He peak. SF₆ and excess ³He concentrations decreased from about 250 ppt (parts per trillion by volume) and $6500 \times 10^{-16} \text{ cm}^3 \text{ STP g}^{-1}$ to about 6 ppt and $6 \times 10^{-16} \text{ cm}^3 \text{ STP g}^{-1}$, respectively. Depth averaged excess ³He/SF₆ ratios decreased from greater than 20 to less than 6 over the course of the experiment (Fig. 3b, Table 1).

Vertical gradients of tracer concentrations were observed. For the first 49 h, surface concentrations were equal to or greater than bottom concentrations in the peak locations. Thereafter, the gradient at peak stations was reversed; bottom SF₆ and excess ³He concentrations were between 0–11% and 4–19% greater than surface concentrations, respectively. Vertical gradients in the ratio of excess ³He/SF₆ were also observed. Ratios in bottom samples were 2–12% greater than ratios in surface samples.

During the first 6 days, samples were collected at approximately slack high tide. The remaining samples were collected at approximately slack low tide. The location of the peak at the same tidal stage moved to the south at a speed of about

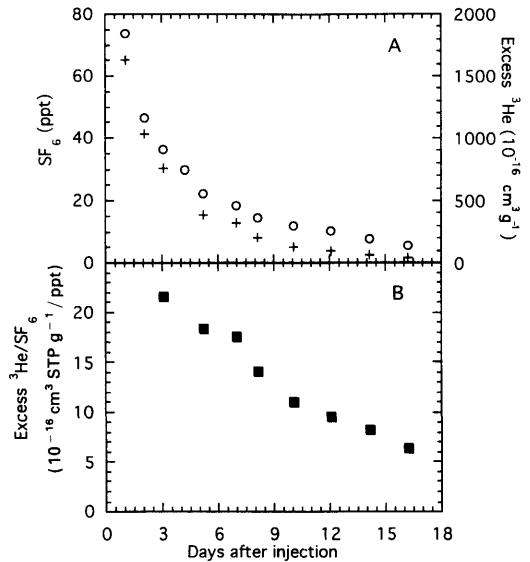


Fig. 3. (a) Decline in peak SF₆ and excess ³He concentration from surface samples with time. The samples collected about 8 h after injection are not plotted. Open circles = SF₆ and crosses = excess ³He. (b) Decline in the depth averaged excess ³He/SF₆ ratio with time. Data collected before the injection depth bias had been removed (before day 3.1) are not included.

1.5 km per day. Peak concentrations were always found between Staatsburg and New Hamburg.

5.2. Wind speeds

All wind speeds recorded during the experiment were corrected to a height of 10 m. This was done by assuming a neutrally stable boundary-layer and a logarithmic wind profile,

$$U_z = (U_* / \kappa) \ln(z/z_o) \quad (5)$$

and

$$U_* = \sqrt{C_d} U_{10}, \quad (6)$$

where U_z is wind speed at height z , U_* is the air friction velocity, κ is the Von Karman constant (0.4), z_o is the surface roughness, and C_d is the drag coefficient assumed to equal 1.3×10^{-3} . U_{10} at the lighthouse were 4% lower than observed values and U_{10} at the buoy were 17% higher than observed values.

After the tracer experiment was completed, the two anemometers were placed about 5 m apart on

Table 1. Results of the tracer experiment

Days after injection	Depth (m)	Peak SF ₆ (ppt)	Concentration excess ³ He (10 ⁻¹⁶ cm ³ STP g ⁻¹)	Average ratio ^{a)}	U ₁₀		k ₆₀₀ ^{c)} (cm h ⁻¹)
					lighthouse (m s ⁻¹)	buoy ^{b)} (m s ⁻¹)	
0.35	1	264	6484				
	10	122	3243				
1.08	1	73.5	1642		4.2		
	14	58.2	1406				
2.04	1	46.3	1040		0.7		
	16	43.0	lost				
3.08	1	36.2	754	21.5	1.6	1.1	
	14	37.2	827				
4.20	1	29.6	lost	—	—	—	
	14	31.4 ^{d)}	591 ^{d)}				
5.19	1	22.3	387	18.4	3.9 ^{e)}	2.2 ^{e)}	3.9 ^{e)}
	19	24.5	476				
7.02	1	18.5	323	17.5 ^{f)}	2.5	1.8	1.5
	n.s. ^{g)}	—	—				
8.15	1	14.5	202	14.1	4.9	3.4	9.0
	12	16.2	230				
10.07	1	11.9	129	11.1	3.1	2.2	6.3
	15	11.9	134				
12.09	1	10.1	97	9.6	3.2	2.6	3.5
	15	10.0	95				
14.15	1	7.6	60	8.2	2.8	2.0	3.6
	17	7.6	67				
16.23	1	5.7	37	6.4	3.2	2.9	5.9
	12	6.1	39				

^{a)} Ratios were calculated by averaging the excess ³He/SF₆ ratio of surface and bottom samples.

^{b)} Buoy wind speeds corrected for the negative offset.

^{c)} k₆₀₀ was calculated using eqs. (2) and (3) from the average ratio assuming the Schmidt number exponent equals $\frac{1}{2}$.

^{d)} Maximum concentrations from different bottom samples.

^{e)} Calculated for the period between day 3.08 and 5.19.

^{f)} Ratio calculated from only the surface sample.

^{g)} A bottom sample was not collected in the peak location during this day.

a tall building. Hourly mean wind speeds were recorded for 48 h. During this period, mean wind speeds ranged between 0.1 and 2.8 m s⁻¹. At these low wind speeds, the 2 anemometers recorded the same mean wind speed each hour ($\pm 3\%$).

However, during the experiment, there appears to have been a negative offset in the wind speeds recorded on the buoy. Instantaneous minimum speeds which were recorded each hour were frequently less than zero (the data logger recorded

negative voltage signals). Furthermore, hourly mean wind speeds corrected to 10 m, U₁₀, recorded on the buoy (2 m) and on the Esopus Meadow Lighthouse (16.5 m) during an 18-h period when the instruments were placed about 200 m apart correlated with a slope of approximately 1 and a non-zero intercept (Fig. 4). A zero intercept can be achieved by adding 0.35 m s⁻¹ to all speeds recorded on the buoy. The non-zero intercept in Fig. 4 does not appear to have resulted from a

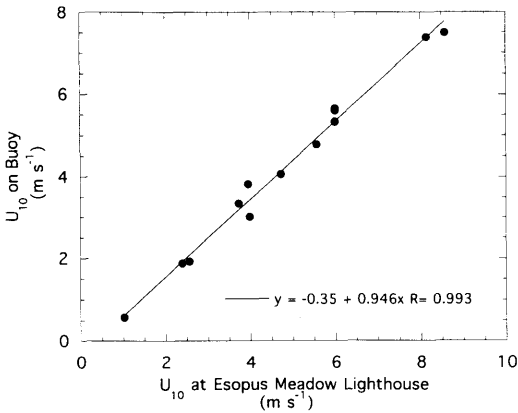


Fig. 4. Hourly mean U_{10} recorded at the buoy and Esopus Meadow Lighthouse plotted against each other recorded while the instruments were about 200 m apart. The U_{10} of the buoy has not been corrected for the negative offset.

higher threshold to get the anemometer spinning on the buoy than on the lighthouse because the same offset was found for each hour despite instantaneous minimum wind speeds which ranged between 0.0 and 3.6 $m s^{-1}$. Unfortunately, we were unable to reproduce the negative offset in the laboratory after the tracer experiment and cannot offer an explanation.

The vertical profile of wind speed at the lighthouse was collected between 5 p.m. and 11 a.m. on 9 and 10 September 1993. Data collected during the 5 h centered around low tides were removed because the buoy was resting on the sediments, causing the anemometer to point significantly away from vertical. The good correlation of U_{10} for the remaining 13 h suggests that our correction method is reasonable.

Hourly mean U_{10} values recorded at the Esopus Meadow Lighthouse ranged from 0.04 to 9.4 $m s^{-1}$ and averaged 3.1 $m s^{-1}$ during our sixteen day experiment (Fig. 5). Mean U_{10} between sampling periods ranged from 0.7 to 5.1 $m s^{-1}$. For the same periods, U_{10} recorded on the buoy and corrected for the negative offset (by adding 0.35 $m s^{-1}$ to all values) correlates with mean U_{10} recorded on the lighthouse, although they were on average 30% lower (Table 1). The good correlation between the two anemometers resulted from the strongly channelized winds along the main axis of the river. About 70% of the time, the hourly prevailing wind

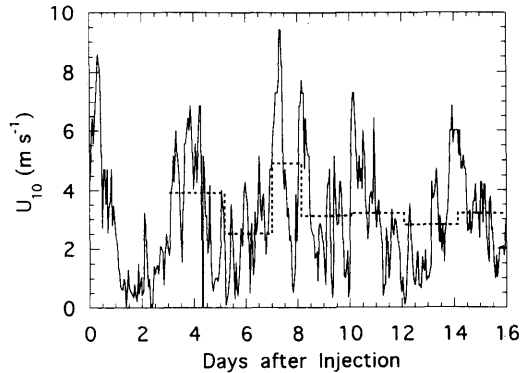


Fig. 5. Mean wind speeds recorded on the Esopus Meadow Lighthouse during the tracer experiment corrected to a height of 10 m. Solid line = hourly mean wind speeds; dashed line = mean winds between sampling events.

direction recorded on the lighthouse was out of the NNE or SSW (Fig. 6).

The lower wind speeds at the buoy may have resulted from its location. The buoy was located in a more sheltered area of the river than the lighthouse between the shore and Esopus Island

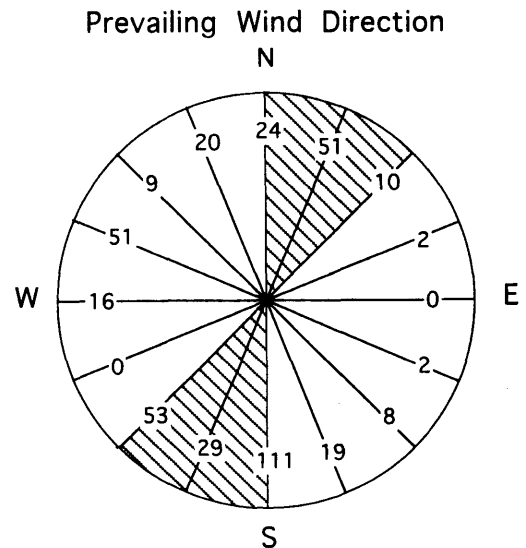


Fig. 6. Prevailing wind direction recorded each hour on the Esopus Meadow Lighthouse. Plotted with each compass direction is the number of hours the prevailing wind was in that direction during the tracer experiment. About 70% of the time the prevailing wind direction occurred in the shaded area.

(Fig. 1). About 3 km to the north and 1 km to the south, points of land extended from the shore past the buoy's location blocking the north-south wind directions. The lower wind speeds could have also resulted from the strong tidal currents which caused the buoy to lean slightly at all times.

Wind speeds over rivers are variable because of local channel effects. The mean wind speeds recorded at the buoy should be representative of more sheltered areas and probably are good estimates of minimum wind speeds. The mean wind speeds recorded on the lighthouse should be representative of the open area of the channel and are probably good estimates of the maximum wind speeds. We estimate that more than 70% of the channel surface area is free of local obstructions and should have wind speeds similar to those recorded on the lighthouse. Hence, the mean wind speeds recorded on the lighthouse should be more representative of the wind field influencing the gas exchange rate than mean wind speeds recorded on the buoy.

5.3. Gas exchange rates

During the entire period of the experiment on the tidal Hudson River, we never observed a vertically homogeneous tracer patch. Vertical gradients were caused by sluggish vertical mixing compared to gas loss across the air-water interface by gas exchange. Because the loss of the injected gases occurred only at the air-water interface, bottom concentrations should be greater than surface concentrations. However, greater surface concentrations of tracers were observed during the first 49 h. The inversion of the gradients was caused by the injection depth which was significantly above the surface of the sediments. After 3 days of mixing, the injection depth bias appears to have been removed and the expected vertical gradients were observed.

To calculate the gas transfer velocity, k , using eqs. (3) and (5), we averaged the excess $^3\text{He}/\text{SF}_6$ ratio of the surface and bottom samples from peak stations. First order gas transfer rates were calculated from the change in the depth averaged ratio with time using eq. (3). The calculated rates were then converted to gas transfer velocities using eq. (5), assuming that change of the bulk water column and surface concentrations (1 m below the air-water interface) between adjacent sampling times were linear as a function of time. In these

calculations, we have assumed that the difference between the tracer concentrations adjacent to the air-water interface and at a depth of 1 m is negligible.

The gas transfer velocities corrected to a Schmidt number of 600 using eq. (2), range between 1.5 and 9.0 cm h^{-1} (Table 1). (In freshwater, the Schmidt number for oxygen at 17.5°C is approximately 600.) In these calculations, the Schmidt number exponent, $\text{Sc}_{(^3\text{He})}$, $\text{Sc}_{(\text{SF}_6)}$, and water temperature were assumed to equal $\frac{1}{2}$, 131, 719, and 26°C, respectively. The average transfer velocities calculated from the change in the depth averaged ratio between day 3.08 and 16.23 was 4.4 cm h^{-1} (mean wind speed at the lighthouse was 3.1 m s^{-1}) assuming the mean and surface concentrations decreased exponentially (Fig. 3a). The correction applied to first-order transfer rates to convert them to gas transfer velocities was small. On average, the product of the first-order transfer rate and mean depth had to be increased by about 5%.

The depth averaged excess $^3\text{He}/\text{SF}_6$ ratio was poorly defined on two transects after the injection depth bias had been removed. On day 4.2, the ^3He sample from the surface station in the peak location was lost during laboratory analysis. Furthermore, maximum concentrations of SF_6 and ^3He occurred in different bottom samples. For these reasons, we have not used this day to calculate gas transfer velocities. No bottom sample was collected at the peak station on day 7.0. We have computed the gas transfer velocity using only the excess $^3\text{He}/\text{SF}_6$ ratio from the surface sample. This ratio should be a minimum value and the gas transfer velocities calculated with the transects collected before and after are maximum and minimum rates, respectively.

5.4. Box model calculations

A simple two-layer box model (Fig. 7) was used to investigate the tracer distributions. In the model description of the Hudson River, the dimensions of surface and bottom boxes were identical, both 7 m deep, 800 m wide, and 500 m long. An average geometry representative of the entire reach for all of the boxes was chosen because of the daily tidal movement of water masses. The tracer patch "feels" approximately 10 km of channel during each tidal cycle. Axial dispersion and net flow downstream were simulated using horizontal (E) and vertical (V) mixing coefficients and the

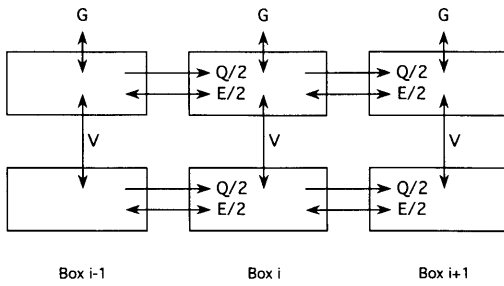


Fig. 7. Drawing of the box model. See the text for a definitions of terms.

freshwater discharge rate (Q). Loss of gas across the air–water interface (G) was calculated from the box surface area, the difference between the box and atmospheric equilibrium concentrations, and the gas transfer velocity which was scaled for each gas according to the Schmidt number dependance (eq. (2)). Tracers were injected into one surface box at time zero. The time step was set equal to 1 h.

We varied the gas transfer velocity during the model calculations to match the inferred changes in the rate we observed during the tracer experiment (Table 2). The amount of tracer added was varied until model calculated tracer concentrations of peak samples matched observed values on day 3.1. The amount of tracers required to reproduce the observed concentrations were 0.13 moles of SF_6 and 0.00036 moles of ^3He . This calculation suggests that about 20% of the SF_6 and 35% of the ^3He dissolved in the water column during the injection with the remainder leaving the water surface in bubbles. Freshwater flow, Q , between the boxes was chosen so that the calculated movement of the tracer peak downstream matched the observations. The peak height, mid-peak width, and vertical gradients of the observed tracer patches were used to constrain the vertical and horizontal mixing rates. The tracer distributions were best matched with horizontal and vertical fluxes of $90 \text{ m}^3 \text{ s}^{-1}$ and $20 \text{ m}^3 \text{ s}^{-1}$, respectively

Table 2. Results of box model calculation

Days after injection	Box ^{a)}	Peak SF_6 (ppt)	Concentration excess ^3He ($10^{-16} \text{ cm}^3 \text{ STP g}^{-1}$)	Average ratio ^{b)}	calculated ^{c)} k_{600} (cm h^{-1})	input ^{d)} (cm h^{-1})
1	S	86.1	2136			3.0
	B	55.2	1460			
3	S	35.2	734	22.0		3.0
	B	36.8	848			
5.2	S	22.9	400	18.6	3.6	3.6
	B	24.8	489			
7	S	19.1	326	17.5	1.3	1.7
	B	19.8	355			
8.2	S	13.4	162	13.9	9.4	9.4
	B	16.3	257			
10	S	10.4	107	11.5	5.9	5.1
	B	12.0	151			
12	S	8.7	81	10.0	3.4	3.3
	B	9.4	100			
14.2	S	7.1	59	8.7	3.0	3.1
	B	7.7	70			
16.2	S	5.3	34	6.9	5.6	5.5
	B	6.1	46			

a) S = surface box; B = bottom box.

b) Ratios were calculated by averaging the excess $^3\text{He}/\text{SF}_6$ ratio of surface and bottom boxes.

c) Gas exchange rates were calculated from the depth averaged ratio listed in the adjacent column using eq. (3).

d) Gas exchange rates specified in the model calculations.

(Table 2). Using the model calculated peak concentrations, we calculated gas exchange rates from the change in the depth averaged excess $^3\text{He}/\text{SF}_6$ ratio using eq. (3). The rates calculated from the model distributions matched the prescribed gas exchange rates (Table 2).

6. Discussion

The gas transfer velocities calculated with eqs. (3) and (5) using the depth averaged excess $^3\text{He}/\text{SF}_6$ ratio correlate well with mean wind speeds, U_{10} , recorded at the lighthouse (Fig. 8). Other gas exchange experiments in tidal waters have also found a strong correlation between mean wind speed and gas exchange rate, although those experiments relied on the "helmet" and mass balance methods (Juliano, 1969; Hartman and Hammond, 1984; Kim and Holley, 1988; Marino and Howarth, 1993). Both the mean gas transfer velocity and wind speed observed during our experiment were significantly lower than mean values determined for the open ocean (Peng et al., 1979; Broecker et al., 1985; Wanninkhof, 1992).

Plotted with the results of our Hudson River tracer experiment in Fig. 8 are trend lines from lake tracer experiments (Wanninkhof et al., 1985;

1987) and the empirical relationship of Liss and Merlivat (1986). Our data agrees well with the trend lines from Rockland (surface area = 1 km²) and Crowley (surface area = 20 km²) Lakes when using the wind data recorded on the Esopus Meadow Lighthouse (Fig. 8). However, if the mean U_{10} recorded at the buoy are used, our gas transfer velocities shift to lower wind speeds and fall above the lake data. The minimum gas transfer velocity observed for the tidal Hudson River agrees with minimum gas transfer velocities observed for lakes during periods of low wind speeds. This suggests that the tidal currents do not add significantly to the surface turbulence field and, hence, do not influence the gas transfer velocity. The relationship of Liss and Merlivat (1986) does not represent the Hudson data well. It predicts lower gas exchange rates than observed.

Earlier measurements of gas exchange rates for the Hudson River have been made by Marino and Howarth (1993) using the "helmet" method. They also found that the gas exchange rate correlated with wind speed although their relationship between gas transfer velocity and wind speed falls above our data when using the U_{10} recorded at the Esopus Meadow Lighthouse. However, their relationship agrees well with our data if we use the lower wind speeds recorded at the buoy. Their anemometer was placed in the main channel, hence their wind data is most comparable to the wind data recorded at the Esopus Meadow Lighthouse. Assuming a mean wind speed of 3.1 m s⁻¹ (the mean wind speed observed at the lighthouse during our experiment), their relationship (see Fig. 3b in Marino and Howarth, 1993) predicts a gas transfer velocity of 5.5 cm h⁻¹ after correcting to a Schmidt number of 600. This rate is approximately 25% higher than the mean gas exchange rate (4.4 cm h⁻¹) we observed during our experiment.

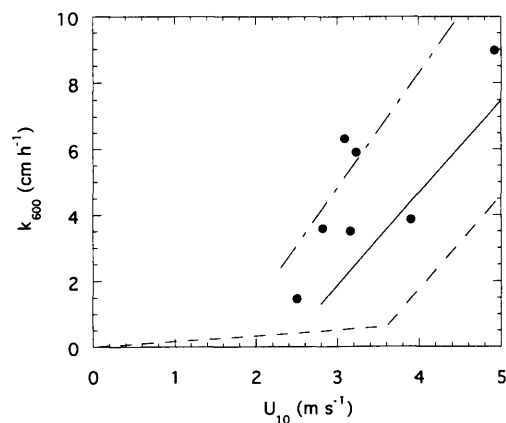


Fig. 8. Mean gas transfer velocities corrected to a Schmidt number of 600, K_{600} , plotted against mean wind speeds recorded at the Esopus Meadow Lighthouse corrected to 10 m, U_{10} . The solid line shows the trend observed in Rockland Lake and the dashed-dotted line shows the trend observed in Crowley Lake (Wanninkhof et al., 1985; 1987). The dashed line shows the empirical relationship of Liss and Merlivat (1986) for steady winds.

7. Conclusions

The $^3\text{He}\text{-SF}_6$ method of determining gas exchange rates has been successfully used in a tidal river. The dispersion and decline of these inert trace gases followed a predictable pattern. One complication observed was related to vertical gradients in tracer concentrations. A small correction had to be applied to the product of the first

order transfer rate and mean depth to convert them to gas transfer velocities. The tracer distributions could be explained entirely by loss across the air-water interface and physical mixing as illustrated by our box model calculations.

The gas exchange rate in the tidal Hudson River was found to correlate with wind speed. Using the mean wind speeds recorded at the Esopus Meadow Lighthouse, the relationship between wind speed and gas transfer velocity falls close to those observed for lakes. Good agreement is also found at low wind speeds, suggesting that the tidal currents are not a dominant influence on the gas exchange rate.

8. Acknowledgements

We wish to thank M. Taylor and S. Chillrud for helping with the field work. C. Weaver and

J. Feeney provided dock space at the Norrie Point Marina and helped keep our boat running. A. Fitzpatrick and W. Spencer granted permission to place anemometers on the Esopus Meadow Lighthouse and in the Poughkeepsie Yacht Club anchorage. Dr. J. Walker provided laboratory space at Vassar College for the SF₆ gas chromatograph. Special thanks go to Dr. R. Hires and Dr. S. Thomas who injected rhodamine WT dye simultaneously with the gases. The dye proved to be very valuable in locating the tracer patch during the first 2 days of the experiment. R. Weppernig, B. Ekwurzel, and E. Kohandoust prepared and measured the ³He samples. The ³He analyses were made possible by a generous donation by the W. M. Keck Foundation. Financial support was provided by the Hudson River Foundation (grant no. 011/92A). This is contribution no. 5191 from the Lamont-Doherty Earth Observatory of Columbia University.

REFERENCES

- Belanger, T. V. and Korzum, E. A. 1991. Critique of floating-dome technique for estimating reaeration rates. *J. Environ. Eng.* **117**, 144–150.
- Broecker, W. S., Peng, T.-H., Ostlung, G. and Struiver, M. 1985. The distribution of bomb radiocarbon in the ocean. *J. Geophys. Res.* **90**, 6953–6970.
- Benson, B. B. and Krause, D., Jr. 1980. Isotopic fractionation of helium during solution: a probe for the liquid state. *J. Solution Chem.* **9**, 895–909.
- Clark, J. F., Simpson, H. J., Smethie, W. M., Jr. and Toles, C. 1992. Gas exchange in a contaminated estuary inferred from chlorofluorocarbons. *Geophys. Res. Lett.* **19**, 1133–1136.
- Clarke, W. B., Jenkins, W. B. and Top, Z. 1976. Determination of tritium by mass spectrometric measurement of ³He. *Int. J. Appl. Radiat. Isotopes* **27**, 217–225.
- De Angelis, M. A. and Scranton, M. I. 1993. Fate of methane in the Hudson River and Estuary. *Global Biogeochem. Cycles* **7**, 509–523.
- Deck, B. L. 1981. *Nutrient-element distributions in the Hudson estuary*. Ph.D. thesis, 396 pp., Columbia Univ., New York.
- Dyrssen, D., Fogelqvist, E., Krysell, M. and Sturm, R. 1990. Release of halocarbons from an industrial estuary. *Tellus* **42B**, 162–169.
- Hammond, D. E., Simpson, H. J. and Mathieu, G. 1977. Radon 222 distribution and transport across the sediment-water interface in the Hudson River estuary. *J. Geophys. Res.* **82**, 3913–3920.
- Hartman, B. and Hammond, D. E. 1984. Gas exchange rates across the sediment-water and air-water interfaces in South San Francisco Bay. *J. Geophys. Res.* **89**, 3593–3603.
- Howarth, R. W., Marino, R., Garritt, R. and Sherman, D. 1992. Ecosystem respiration and organic carbon processing in a large, tidally influenced river: the Hudson River. *Biogeochem.* **16**, 83–102.
- Jähne, B., Munnich, K. O., Bosinger, R., Dutzi, A., Huber, W. and Libner, P. 1987. On parameters influencing air-water gas exchange. *J. Geophys. Res.* **92**, 1937–1949.
- Juliano, D. W. 1969. Reaeration measurements in an estuary. *J. of San. Eng. Div. ASCE* **95**, 1165–1178.
- Kim, J. H. and Holley, E. R. 1988. *Literature survey on reaeration in estuaries*. Technical Memorandum 88-1. Center for Research in Water Resources, University of Texas. 75 p.
- Limburg, K. E., Moran, A. and McDowell, W. H. 1986. *The Hudson river ecosystem*. Springer-Verlag, NY, 331 p.
- Liss, P. S. and Merlivat, L. 1986. Air-sea gas exchange rates: Introduction and synthesis. In: *The rôle of air-sea exchange in geochemical cycling* (ed. P. Buat-Ménard). D. Reidel, Norwell, Mass., 113–127.
- Marino, R. and Howarth, R. W. 1993. Atmospheric oxygen exchange in the tidal Hudson River: Dome measurements and comparison with other natural waters. *Estuaries* **16**, 433–445.
- O'Loughlin, E. M. and Bowmer, K. H. 1975. Dilution of aquatic herbicides in flowing channels. *J. of Hydrol.* **26**, 217–235.
- Peng, T.-H., Broecker, W. S., Mathieu, G. and Li, Y.-H.

1979. Radon evasion rates in the Atlantic and Pacific oceans as determined during GEOSECS program. *J. Geophys. Res.* **84**, 2471–2486.
- Stephens, D. W. 1978. Preliminary evaluation of the floating dome method of measuring reaeration rates. *J. of Res. of U. S. Geol. Surv.* **6**, 547–552.
- Thomann, R. V., Mueller, J. A., Winfield, R. P. and Huang, C.-R. 1991. Model of fate and accumulation of PCB homologues in Hudson Estuary. *J. Envir. Eng.* **117**, 161–178.
- Upstill-Goddard, R. C., Watson, A. J., Liss, P. S. and Liddicoat, M. I. 1990. Gas transfer velocities in lakes measured with SF₆. *Tellus* **42B**, 364–377.
- Wanninkhof, R. 1992. Relationship between gas exchange and wind speed over the ocean. *J. Geophys. Res.* **97**, 7373–7381.
- Wanninkhof, R., Ledwell, J. R. and Broecker, W. S. 1985. Gas exchange-wind speed relationship measured with sulfur hexafluoride on a lake. *Science* **227**, 1224–1226.
- Wanninkhof, R., Ledwell, J. R., Broecker, W. S. and Hamilton, M. 1987. Gas exchange on Mono Lake and Crowley Lake, California. *J. Geophys. Res.* **92**, 14567–14580.
- Wanninkhof, R., Asher, W., Weppernig, R., Chen, H., Schlosser, P., Langdon, C. and Sambrotto, R. 1993. Gas transfer experiment on Georges Bank using two volatile deliberate tracers. *J. Geophys. Res.* **98**, 237–248.
- Watson, A. J., Upstill-Goddard, R. C. and Liss, P. S. 1991. Air-sea exchange in rough and stormy sea, measured by a dual tracer technique. *Nature* **349**, 145–147.
- Weiss, R. 1971. Solubility of helium and neon in water and seawater. *J. Chem. Eng. Data* **16**, 235–241.